Am J Physiol Cell Physiol 286: C1109–C1117, 2004.
First published December 24, 2003; 10.1152/ajpcell.00183.2003.

Effects of cytochrome *c* on the mitochondrial apoptosis-induced channel MAC

Liang Guo,[1] Dawn Pietkiewicz,[1] Evgeny V. Pavlov,[1] Sergey M. Grigoriev,[1] John J. Kasianowicz,[2] Laurent M. Dejean,[1] Stanley J. Korsmeyer,[3] Bruno Antonsson,[4] and Kathleen W. Kinnally[1]

[1]*Department of Basic Sciences, College of Dentistry, New York University, New York, New York 10010;* [2]*Biotechnology Division, National Institute of Science and Technology, Gaithersburg, Maryland 20899-8313;* [3]*Departments of Pathology and Medicine, Harvard Medical School, Dana-Farber Cancer Institute, Howard Hughes Medical Institute, Boston, Massachusetts 02115; and* [4]*Serono Pharmaceutical Research Institute, Serono International, CH-1228 Plan-les Ouates, Geneva, Switzerland*

Submitted 6 May 2003; accepted in final form 10 December 2003

Guo, Liang, Dawn Pietkiewicz, Evgeny V. Pavlov, Sergey M. Grigoriev, John J. Kasianowicz, Laurent M. Dejean, Stanley J. Korsmeyer, Bruno Antonsson, and Kathleen W. Kinnally. Effects of cytochrome *c* on the mitochondrial apoptosis-induced channel MAC. *Am J Physiol Cell Physiol* 286: C1109–C1117, 2004. First published December 24, 2003; 10.1152/ajpcell.00183.2003.—Recent studies indicate that cytochrome *c* is released early in apoptosis without loss of integrity of the mitochondrial outer membrane in some cell types. The high-conductance mitochondrial apoptosis-induced channel (MAC) forms in the outer membrane early in apoptosis of FL5.12 cells. Physiological (micromolar) levels of cytochrome *c* alter MAC activity, and these effects are referred to as types 1 and 2. Type 1 effects are consistent with a partitioning of cytochrome *c* into the pore of MAC and include a modest decrease in conductance that is dose and voltage dependent, reversible, and has an increase in noise. Type 2 effects may correspond to "plugging" of the pore or destabilization of the open state. Type 2 effects are a dose-dependent, voltage-independent, and irreversible decrease in conductance. MAC is a heterogeneous channel with variable conductance. Cytochrome *c* affects MAC in a pore size-dependent manner, with maximal effects of cytochrome *c* on MAC with conductance of 1.9–5.4 nS. The effects of cytochrome *c*, RNase A, and high salt on MAC indicate that size, rather than charge, is crucial. The effects of dextran molecules of various sizes indicate that the pore diameter of MAC is slightly larger than that of 17-kDa dextran, which should be sufficient to allow the passage of 12-kDa cytochrome *c*. These findings are consistent with the notion that MAC is the pore through which cytochrome *c* is released from mitochondria during apoptosis.

patch clamp; ion channels

APOPTOSIS IS A PHENOMENON fundamental to higher eukaryotes and essential to the mechanisms underlying tissue homeostasis. The pro- and antiapoptotic members of the Bcl-2 family control the release of cytochrome *c* and other factors from mitochondria (38). The release of cytochrome *c* from mitochondria is considered the commitment step of apoptosis in many cell types (17, 23, 37, 38). Cytochrome *c* binds APAF-1 and procaspase-9 in the presence of dATP to form the apoptosome complex. The apoptosome then activates caspase-3, and the degenerative stage of apoptosis begins (23). It has been proposed that cytochrome *c* release results from the rupture of the mitochondrial outer membrane after opening of the permeability transition pore (5, 20). In contrast, recent investigations support the notion that cytochrome *c* exits directly through a pore in the mitochondrial outer membrane without loss of outer membrane integrity (2, 5, 9, 28, 30, 33, 34). Hence, the mechanism of cytochrome *c* release is not well understood.

A novel, high-conductance channel forms in the mitochondrial outer membrane early in apoptosis and was discovered by applying patch-clamp techniques to mitochondria isolated from apoptotic FL5.12 cells (30). The appearance of the mitochondrial apoptosis-induced channel (MAC) is prevented by overexpression of Bcl-2 (30). The single-channel activity of the MAC is examined by patch clamping proteoliposomes containing mitochondrial outer membranes isolated from apoptotic cells. The average diameter of the pore of MAC is ~4 nm when calculated from its typical peak, single-channel transition size of ~2.5 nS, but the pore may be even larger. Therefore, MAC may provide a pathway for cytochrome *c* and even larger proteins to escape from the space between the mitochondrial membranes early in apoptosis. Previously, the failure of proteoliposomes containing MAC to retain cytochrome *c* provided indirect evidence that cytochrome *c* may cross the mitochondrial outer membrane via MAC (30). Here, modification of the electrophysiological activity of MAC by cytochrome *c* provides direct evidence that cytochrome *c* partitions into the pore of MAC, consistent with the notion that MAC mediates release of cytochrome *c* from mitochondria early in apoptosis. Similar direct evidence of transport has also been reported for the effect of ATP on voltage-dependent anion-selective channels (VDAC) (31) and RNA on α-hemolysin channels (1, 15).

MATERIALS AND METHODS

Cells and growth conditions. Parental FL5.12 cells were cultured as previously described (10) in Iscove's modified Eagle's medium (IMEM), 10% fetal bovine serum, and 10% WEHI-3B supplement (filtered supernatant of WEHI-3B cells secreting IL-3). FL5.12 clones overexpressing Bcl-2 or Bcl-2 mutant (G145E substitution) were passed in this medium plus 1 mg/ml Geneticin (G418) (39). Cultures were kept at $<1.5 \times 10^6$ cells/ml. Cells were washed three times in medium with (control) or without (apoptotic) IL-3 (WEHI supplement) 12 h before isolation of mitochondria.

Isolation of mitochondria and preparation of proteoliposomes. Mitochondria were isolated from 2–15 g of FL5.12 cells as previously described for outer membrane preparations (24, 30). Mitochondrial outer membranes were stripped from inner membranes by French pressing isolated mitochondria using modifications of the method of Decker and Greenawalt (8). French pressing was done at 2,000 psi in 460 mM mannitol, 140 mM sucrose, 2 mM EDTA, and 10 mM HEPES, pH 7.4. The pressed suspension was diluted 1:1 with 230 mM mannitol, 70 mM sucrose, 1 mM EDTA, and 5 mM HEPES, pH 7.4,

Address for reprint requests and other correspondence: K. W. Kinnally, Dept. of Basic Sciences, College of Dentistry, New York Univ., 345 East 24th St., New York, NY 10010 (E-mail: kathleen.kinnally@nyu.edu).

The costs of publication of this article were defrayed in part by the payment of page charges. The article must therefore be hereby marked "*advertisement*" in accordance with 18 U.S.C. Section 1734 solely to indicate this fact.

Downloaded from http://ajpcell.physiology.org/ by 10.220.32.246 on October 13, 2017

and centrifuged at 15,000 rpm for 15 min. Outer membranes were separated from inner membranes as described by Mannella and colleagues (26, 27).

Proteoliposomes were formed by a modification of the method of Criado and Keller (7) and Lohret et al. (24). Briefly, small liposomes were formed by sonication of lipid (type IV-S soybean L-α-phosphatidylcholine; Sigma) in water. Sonication was carried out at power setting 7 with a Fisher 60 Sonic dismembrator and attached ultrasonic converter for 30 s on and 30 s off, for a total of 10 min, on ice. Small liposomes were centrifuged at 45,000 rpm for 2 h with an MLA-80 rotor in a Beckman Optima ultracentrifuge. Mitochondrial outer membranes (30–35 μg protein) and small liposomes (600 μg lipid) were mixed with 5 mM HEPES, pH 7.4 (50 μl final volume), and dotted (~0.5-μl dots) on a glass slide. Samples were dehydrated (~3 h) and rehydrated overnight with 150 mM KCl and 5 mM HEPES, pH 7.4 (rehydration medium) at 4°C. Proteoliposomes were harvested with ~0.5 ml of rehydration medium and stored at −80°C.

Time-lapse microscopy. Cells were grown as described above and incubated on slides coated with Cell-Tak (Becton Dickinson). Slides were mounted in sealed Rose chambers maintained at 37°C with IMEM with or without IL-3. Images were taken every 10 min for ~75 h with a Spot RT monochrome charge-coupled device camera (Diagnostics Instruments) on a Nikon Eclipse TE300 phase-contrast microscope, with media exchanges every 24 h. Spot RT software or Scion Imaging (National Institutes of Health) controlled the Uniblitz shutter (model VMMD1). Pictures were captured and then stacked by Scion Imaging or Spot software.

Flow cytometry. Cells were grown and resuspended with or without IL-3 as described above. After 12, 24, 36, and 48 h, cells were harvested at 1,000 *g* for 5 min. Cells were washed in cold PBS twice and resuspended at 2×10^6 cells/ml in 10 mM HEPES, 140 mM NaCl, and 2.5 mM $CaCl_2$, pH 7.4. Cells (4×10^5) were incubated with annexin V according to PharMingen protocol and incubated at room temperature for 15 min. Cells were treated with propidium iodide (Sigma) just before flow cytometry readings. Data were taken for 1×10^4 cells in FACSort (Becton Dickinson) and analyzed by WinMDI software.

Immunoblotting. Proteins were separated by SDS-PAGE and electrotransferred onto polyvinylidene difluoride membranes. Indirect immunodetection employed chemiluminescence (Amersham) with horseradish peroxidase-coupled secondary antibodies. Mitochondrial outer membrane proteins (0.5–2 μg/lane) were probed with primary antibodies against mammalian VDAC (1:2,500; Calbiochem) and Bcl-2 (1:5,000; Research Diagnostics) and a secondary anti-rabbit or anti-mouse antibody (1:5,000; Jackson Immunoresearch).

Patch-clamp analysis. Patch-clamp procedures and analysis were previously described (24, 30). Briefly, membrane patches were excised from proteoliposomes containing purified mitochondrial outer membranes after formation of a gigaseal using micropipettes with ~0.4-μm-diameter tips and resistances of 10–20 MΩ at room temperature. Unless otherwise stated, the solution was symmetrical 150 mM KCl and 5 mM HEPES, pH 7.4. Ion selectivity was determined from the reversal potential after perfusion of the bath with 30 mM KCl, 56 mM sucrose, 184 mM mannitol, and 5 mM HEPES, pH 7.4. Agar bridges were routinely used. Voltage clamp was performed with the excised configuration of the patch-clamp technique (12) by using a Dagan 3900 patch-clamp amplifier in the inside-out mode or an Axopatch 200 amplifier. Voltages are reported as bath potentials. The conductance was typically determined from total amplitude histograms of 30 s of current traces at +20 mV. The pore diameter of MAC

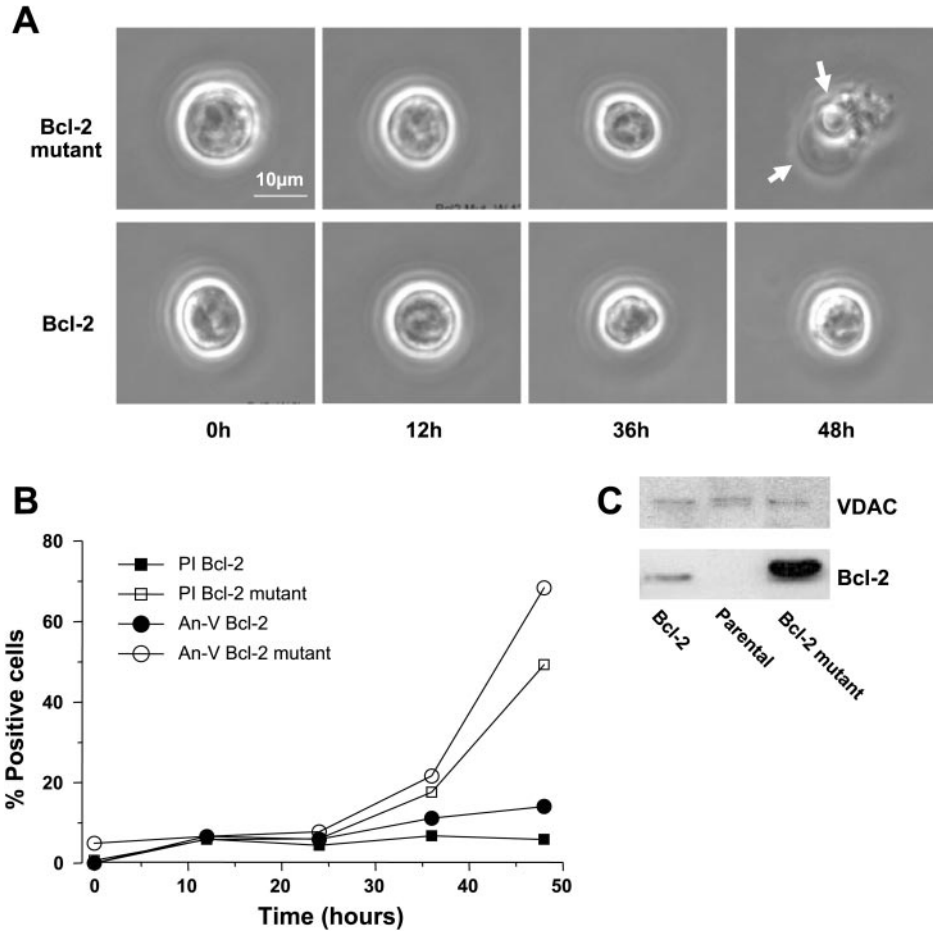

Fig. 1. Onset of apoptosis markers induced by withdrawal of IL-3 and prevented by Bcl-2 overexpression in FL5.12 cells. *A*: sequential images collected with time-lapse video microscopy of cells overexpressing mutant or normal Bcl-2. After IL-3 withdrawal, Bcl-2 mutant cells (*top*) display apoptotic morphological changes, including cell shrinkage (12 h) and membrane blebbing (arrows at 48 h). Overexpression of competent Bcl-2 delays the onset of blebbing (*bottom*). *B*: percentage of positive cells that lost lipid bilayer asymmetry as indicated by annexin V (An-V) labeling and plasma membrane integrity indicated by propidium iodide (PI) labeling as a function of time. *C*: immunoblot showing relative expression levels of Bcl-2 in Bcl-2-overexpressing, Bcl-2 mutant, and parental cell lines relative to the voltage-dependent anion-selective channel (VDAC), the loading control. Although it is almost undetectable in these blots, Bcl-2 is expressed at low levels in parental cells.

Downloaded from http://ajpcell.physiology.org/ by 10.220.32.246 on October 13, 2017

was estimated by using the method of Hille (13) from the peak conductance (reciprocal of the pore resistance) with the assumption that pore length was 5.5 nm (25); i.e., $R_{channel} = \rho(l/\Pi a^2)$, where R and ρ are the resistivity of the pore and solution, respectively, l is pore length, and a is pore radius. Alternatively, the following formula for pore size, which includes access resistance, is $R_{channel} = [l + (\Pi a)/2](\rho/\Pi a^2)$. Dextran solutions were made as 5% (wt/vol, i.e., 5 g of dextran were added to 100 ml) in 150 mM KCl and 5 mM HEPES, pH 7.4. Conductivity of each solution was measured with a Thermo Orion 105 at room temperature. The conductivity ratio of the KCl solution to 5% dextran solutions was 1:0.865, regardless of the size of the dextran molecule. WinEDR version 2.3.3, part of Strathclyde Electrophysiological Software (courtesy of J. Dempster, University of Strathclyde, UK), was used for the variance analysis of noise.

RESULTS

Onset of apoptotic markers in FL5.12 cells after growth factor withdrawal. Apoptosis was induced by withdrawal of IL-3 from three hematopoietic FL5.12 cell lines: parental, Bcl-2-overexpressing (Bcl-2), and mutant (incompetent) Bcl-2-overexpressing cells (10, 29, 39). Bax translocates to the mitochondrial outer membrane and cytochrome *c* is released from mitochondria 12 h after IL-3 withdrawal (10). By this time, the mean diameter of the cells has shifted from 11 μm (normal) to 9 μm, regardless of Bcl-2 level (Fig. 1*A*). Time-lapse video microscopy was used to monitor the morphological changes during apoptosis and the onset of active blebbing, a late marker for apoptosis. Onset of blebbing occurred at 39.5 ± 1 h (n = 26 cells) after IL-3 withdrawal in the Bcl-2 mutant cells (Fig. 1*A*). The same results were obtained with the parental cells (not shown). Bcl-2 overexpression delays apoptosis, inasmuch as cells that overexpress wild-type Bcl-2 were not blebbing before 64 h (Fig. 1*A*). Annexin V labeling of cells indicates a loss of lipid bilayer asymmetry, inasmuch as external annexin V binds to phosphatidylserine, which is normally found exclusively on the inner face of the plasma membrane. Propidium iodide labeling of cells indicates loss of the integrity of the plasma membrane and cell death. Figure 1*B* shows that the onset of propidium iodide and annexin V labeling of cells began ~36 h after IL-3 withdrawal, and overexpression of wild-type Bcl-2 delayed onset of both of these markers of

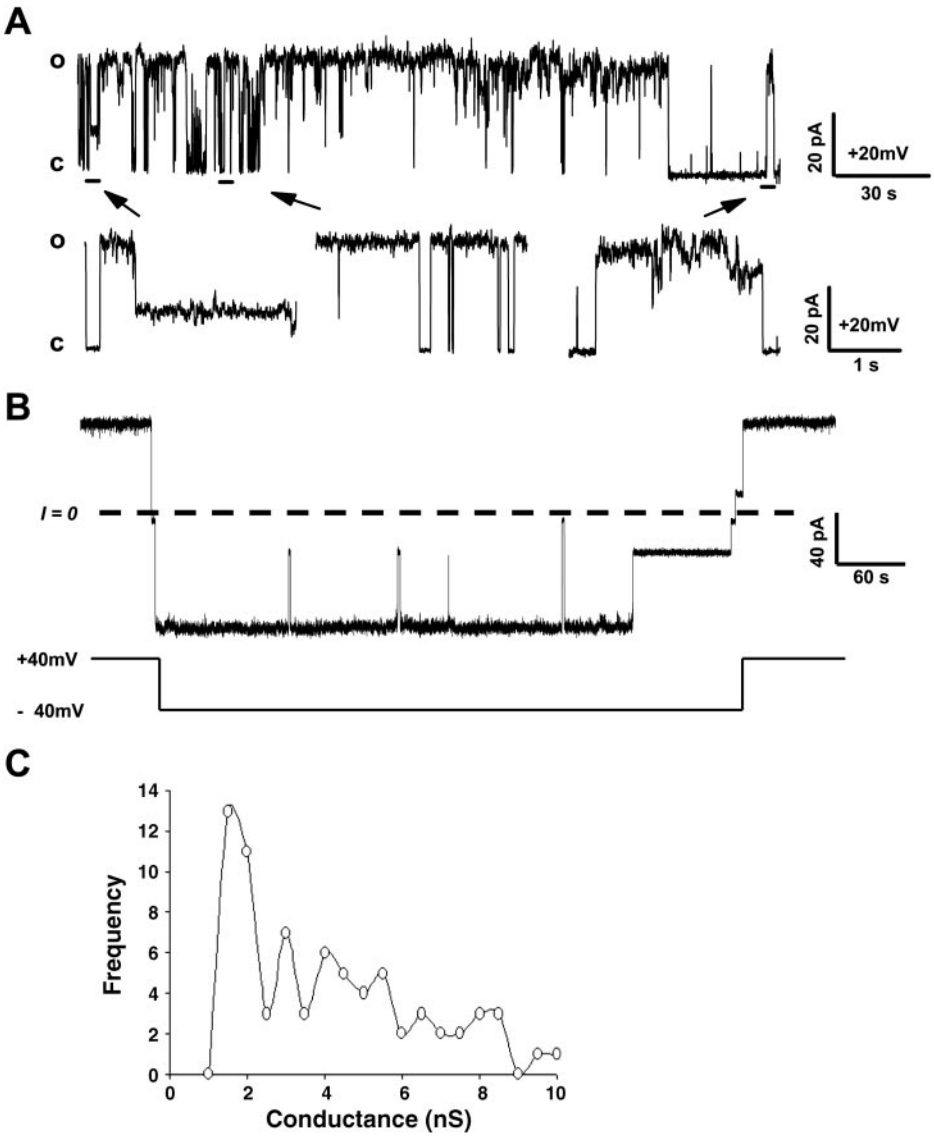

Fig. 2. Mitochondrial apoptosis-induced channel (MAC) is a heterogeneous, high-conductance channel. MAC activity was recorded from proteoliposomes formed by fusion of liposomes with mitochondrial outer membranes of apoptotic FL5.12 cells purified 12 h after IL-3 withdrawal. *A*: current trace at +20 mV illustrating fast kinetic behavior of MAC. This channel displays ~2.1-nS peak transitions and ≥3 sublevel conductance states. *Top traces* were filtered at 10 Hz with 200-Hz sampling; expanded traces (indicated by arrows) were filtered at 2 kHz with 5-kHz sampling. c and o, Closed and open conductance states. *B*: current trace (5-kHz sampling and 2-kHz low-pass filtration) showing MAC with slow kinetics and a long-lived open state. This channel has ~2-nS peak transitions and a sustained open state when voltage clamped at +40 mV. Potential was briefly paused at 0 mV [zero current level (I = 0)] during voltage shifts from +40 to −40 mV and again to +40 mV. *C*: total conductance of MAC shown as a function of frequency of detection in independent patches. Bins are 0.5 nS. Conductances ≤1 nS are not considered to be MAC; this bin is arbitrarily assigned to zero. Total conductance was calculated from total amplitude histograms usually of 30 s of current traces at +20 mV and was not leak subtracted.

Downloaded from http://ajpcell.physiology.org/ by 10.220.32.246 on October 13, 2017

apoptosis. As expected, the Bcl-2 levels were higher in the overexpressing cell lines than the in the parental cells (Fig. 1*C*). MAC activity is detected early in the process of apoptosis (12 h) of parental and mutant Bcl-2 cells but is never found in the wild-type Bcl-2-overexpressing cells (30).

MAC is a heterogeneous high-conductance channel found in apoptotic FL5.12 cells. The permeability of the mitochondrial outer membrane of apoptotic cells increases 12 h after IL-3 withdrawal (30), which is early in apoptosis, before loss of bilayer asymmetry or onset of blebbing (Fig. 1) (30). The single-channel activity of MAC is studied here in proteoliposomes formed by the fusion of small liposomes with outer membranes purified from mitochondria isolated from apoptotic parental FL5.12 cells 12 h after withdrawal of IL-3.

MAC is a heterogeneous channel with a variable high conductance and several substates (Fig. 2). MAC is differentiated from the activities of the two other high-conductance channels of the outer membrane, VDAC and translocase outer membrane (TOM) channel, by single-channel characteristics, including conductance, transition size, voltage dependence, and long open times (30). Conductances below 1.5 nS were not characterized in this study.

The single-channel kinetics of MAC can be classified as fast (rapidly flickering between conductance states) or relatively stable, with a mean open time of minutes. Figure 2*A* shows a current trace of MAC with fast kinetics. This channel frequently fluctuates between the fully open and closed states, with a maximal single transition size of 2.1 nS and at least three substates. Generally, MAC with fast kinetics inactivates quickly or enters the long-lived, fully open state that rarely closes (Fig. 2*B*). The significance of these two different kinetic behaviors is not known and requires further examination. MAC is not typically voltage dependent, because the transitions typically occur randomly. The behavior of each MAC is routinely characterized before effectors are tested. The conductance of MAC is variable (Fig. 2*C*), but conductances of 1.5–5 nS have the highest frequency and are considered the most common.

Effects of cytochrome c on MAC activity. Cytochrome *c* is the best-characterized proapoptotic factor among those normally located in the intermembrane space of mitochondria and released to cytosol early in apoptosis. If cytochrome *c* passes through MAC, changes in MAC activity are expected, because cytochrome *c* has a molecular weight of 12,400 and is positively charged at physiological pH (pI = 10.7) (6). MAC with fast kinetics is not stable for long periods of time. Therefore, the effect of cytochrome *c* was tested on MAC with long-lived openings. Cytochrome *c* reduced the current flow through MAC (Fig. 3). In about half the patches in which cytochrome *c* had an effect, a modest (5–25%) decrease in conductance was observed. These patches typically exhibit rectification, because the current reduction at bath positive potentials was greater than that at negative potentials (Fig. 3*C*). These effects of cytochrome *c* were typically reversible (not shown) and were accompanied by an increase in noise. This increase was evidenced by an approximate doubling of the width of the current traces, which was apparent in the presence of cytochrome *c* (150 mM KCl; Fig. 3, *A* and *B*). The normalized statistical variance of the ionic current increased (189 ± 24%) on introduction of cytochrome *c* to patches containing MAC. In contrast, no cytochrome *c*-induced noise was observed with VDAC or TOM channels (not shown). We refer to the effects of cytochrome *c* on MAC activity that include a modest

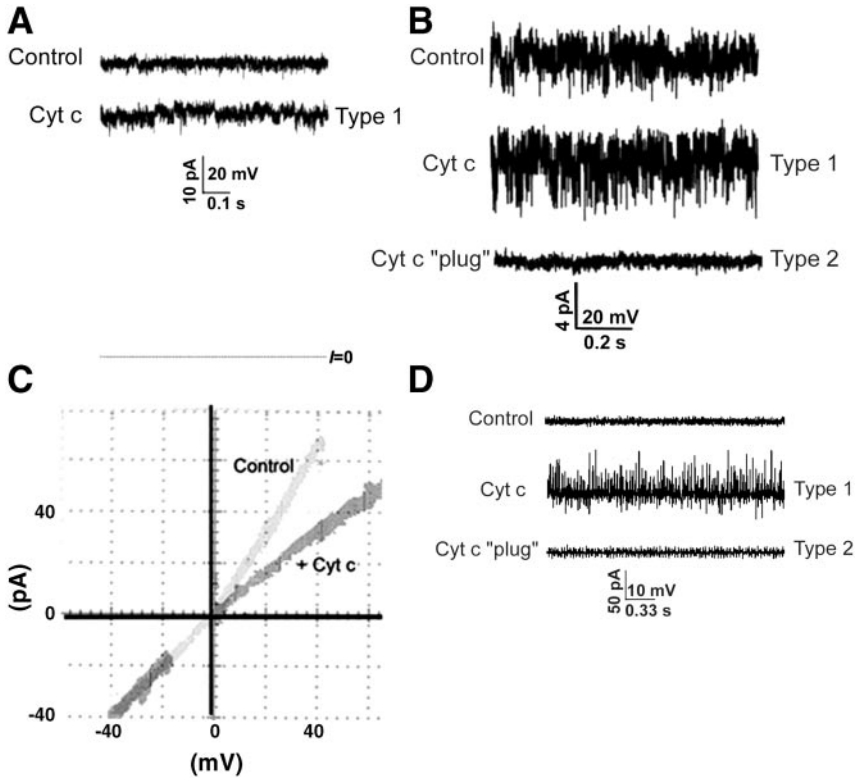

Fig. 3. Effects of cytochrome *c* on conductance and noise level of MAC activity. Type 1 effects are illustrated by current traces of 2 different patches (*A* and *B*) with MAC activity in the absence (control) and presence of 100 μM cytochrome *c* (Cyt *c*). In *A*, $I = 0$. In *B*, mean current levels of control, Cyt *c*, and Cyt *c* "plug" are 56, 54, and 19 pA, respectively (determined by total-amplitude histograms). Current level remained at 54 pA (Cyt *c*) for ~74 s after perfusion with cytochrome *c* and then spontaneously decreased to 19 pA (Cyt *c* "plug"), illustrating a likely shift from type 1 to type 2 effects of cytochrome *c*. Sampling was at 2 kHz with 1-kHz filtration. *C*: current-voltage relation for MAC in the presence (+Cyt *c*) and absence (control) of 100 μM cytochrome *c*. Voltage was manually ramped. In *A–C*, medium was symmetrical 150 mM KCl and 5 mM HEPES, pH 7.4. *D*: discontinuous current traces of the same MAC show activity before and after 100 μM Cyt *c* was introduced into the bath by perfusion. Medium was symmetrical 500 mM KCl and 5 mM HEPES, pH 7.4. Immediately after perfusion, high noise level and modest current decrease (type 1) were spontaneously followed by a further decrease in current and noise (type 2). Mean current levels of the control, Cyt *c*, and Cyt *c* "plug" traces are 230, 175, and 3 pA, respectively. Effect was not reversible, inasmuch as multiple washes for >30 min with medium without cytochrome *c* did not increase current (not shown).

Downloaded from http://ajpcell.physiology.org/ by 10.220.32.246 on October 13, 2017

decrease in conductance that is voltage dependent, reversible, and accompanied by an increase in noise as type 1 effects.

The effect of cytochrome *c* on MAC is variable in magnitude, which suggests that more than one phenomenon is involved, e.g., partitioning of cytochrome *c* into the pore (type 1) and a possible plugging of MAC's pore by cytochrome *c* (type 2). The type 1 effects are described above. The type 2 effects are characterized by a decrease in MAC conductance of >50% (Fig. 4*A*). Type 2 effects were observed in approximately half of the patches in which cytochrome *c* had an effect. This effect of cytochrome *c* on the current through MAC was dose dependent from 10 to 1,000 μM (Fig. 4*B*), which is in the physiological range. The concentration of cytochrome *c* is normally 300–700 μM in the intermembrane space (11). Unlike type 1, the type 2 effects of cytochrome *c* on MAC are not voltage dependent, inasmuch as there is no rectification. As the cytochrome *c* concentration was varied, the current through this MAC was approximately the same at +20 and −20 mV, as shown in the discontinuous current traces of Fig. 4*B*. The noise often decreases with the type 2 effect as the variance of the current traces showing a cytochrome *c* "plug" overlaps that of the control (see also Fig. 3*B*, compare thickness of the current traces). Furthermore, the type 2 effects are typically not reversible, suggesting that there has been a destabilization of the open state, a stabilization of a low-conductance level, or a plugging of the conductance pathway. We are unable to distinguish between these possibilities. Cytochrome *c* may bind or accumulate in the vicinity of the pore of MAC to induce these effects. In summary, the type 2 effects include a large decrease in conductance that is dose dependent, but not voltage dependent, and usually not reversible.

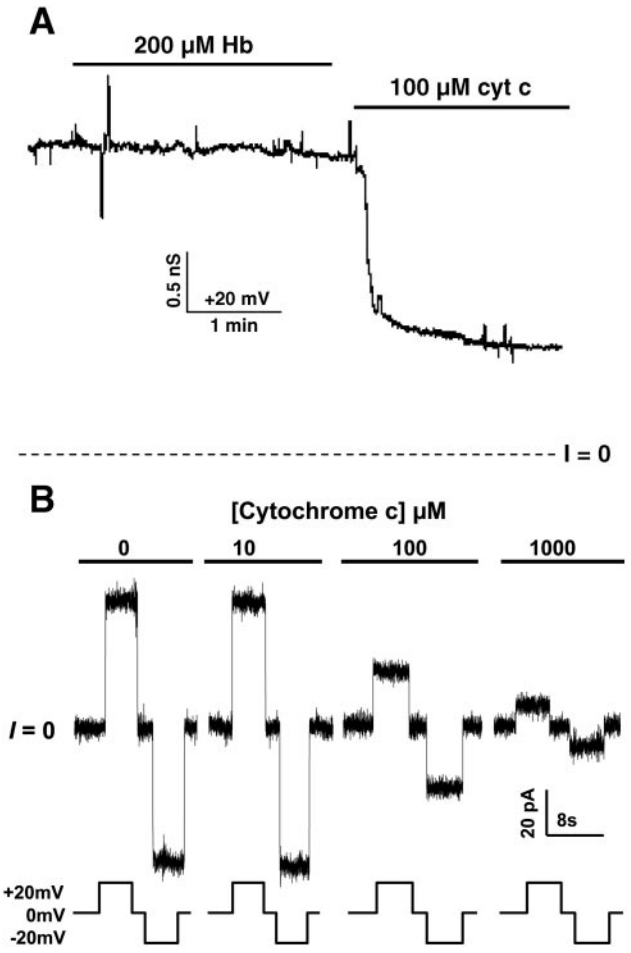

Fig. 4. Type 2 effects of cytochrome *c* on MAC. *A*: current trace of 1 patch in which MAC was recorded at +20 mV before and after application of 200 μM hemoglobin (Hb) and then 100 μM cytochrome *c* (Cyt *c*) illustrates type 2 effect of cytochrome *c* (200-Hz sampling and 10-Hz filtration). Bars above current trace indicate sequential application by perfusion of the bath. $I = 0$ is shown. Large spikes in current are due to perfusion of the bath. *B*: discontinuous current traces of 1 patch with MAC activity with an initial conductance of ~2.6 nS after sequential perfusions of the bath with 0–1,000 μM cytochrome *c* and indicated voltages (5-kHz sampling and 2-kHz filtration). Breaks in current traces indicate short pauses during perfusion.

The possibility that fixed charge and/or the presence of a heme group are important to the effects of cytochrome was examined. The effect of fixed charges on the effects of cytochrome *c* was determined by increasing the concentration of KCl in the bath and pipette media from 150 to 500 mM. Interestingly, the type 1 and type 2 effects of cytochrome *c* on MAC were observed when the ionic strength was increased to reduce ionic interactions. A slight decrease in conductance and a large increase in noise were immediately observed on introduction of 100 μM cytochrome *c* into the bath (typical of type 1 effects) at 500 mM KCl (Fig. 3*D*). Within 1 min, the conductance spontaneously decreased and the noise disappeared (type 2 effects). This effect was not reversed after multiple perfusions of the bath with 500 mM KCl medium without cytochrome *c* for >30 min in this patch. The type 2 effects are apparently not reversible at normal and high ionic strength. The contribution of the heme group to the effects of cytochrome *c* was tested using hemoglobin [molecular weight (dimer) is 32,000 in solution (35)]. Perfusion of the bath with medium containing 200 μM hemoglobin on a patch containing MAC activity did not significantly modify the conductance or noise level (Figs. 4*A* and 5*A*). Therefore, charge and the presence of a heme group are not central to the effects of cytochrome *c* on MAC.

The possibility that the pore size of MAC was responsible for the variability of the effect was explored. MAC is a heterogeneous channel with a variable high conductance and several substates (Fig. 2). In Fig. 5*B*, the magnitude of the effect of cytochrome *c* is indicated as the relative conductance of MAC (conductance with or without cytochrome *c*) in individual patches and is plotted as a function of MAC conductance. No attempt was made to distinguish between type 1 and type 2 effects in this plot. The magnitude of the effect of cytochrome *c* was maximal when the conductance of MAC was 1.9–5.4 nS. The effect of cytochrome *c* when the conductance of MAC was 1.9–5.4 nS was significantly different from that when the conductance was outside this range when these data were binned (Fig. 5*C*). Importantly, cytochrome *c* had no effect on the conductance of VDAC or TOM channel activities and did not change the conductance of liposome patches containing no channel activity (Fig. 5*A*).

MAC is modified by ribonuclease A. The size of the effector may be a crucial determinant of whether there will be a decrease in MAC conductance, because cytochrome *c*, but not hemoglobin, reduced the current flow through MAC at normal (Fig. 4*A*) and high ionic strength (Fig. 3*D*; hemoglobin not shown). Ribonuclease A is slightly larger (13.7 kDa) and slightly less positively charged than cytochrome *c* at neutral pH

Downloaded from http://ajpcell.physiology.org/ by 10.220.32.246 on October 13, 2017

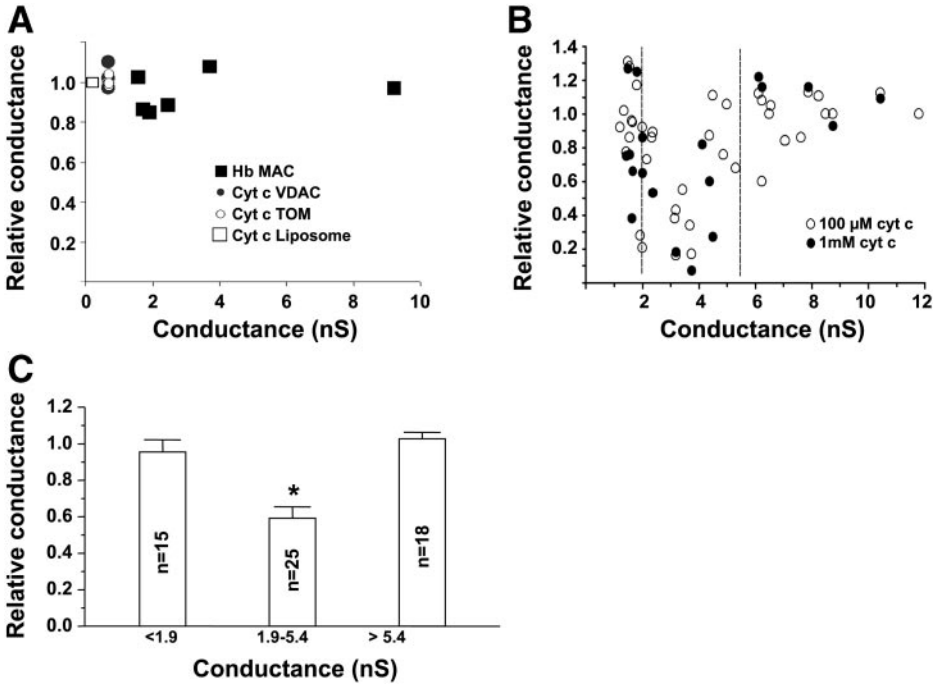

Fig. 5. Cytochrome *c* effects vary with MAC conductance. *A*: conductance of MAC, VDAC, and translocase outer membrane (TOM) channels was determined from total amplitude histograms of typically 30 s of current traces at +20 mV in the presence and absence of 100 μM cytochrome *c* or 200 μM hemoglobin. Relative conductance (conductance in the presence of effector normalized to conductance in the absence of effector) is plotted as a function of channel conductance. Each point indicates a single determination. *B*: relative conductance of MAC (determined as described in *A*) with 100 μM or 1 mM cytochrome *c* as a function of MAC conductance. Each point indicates a single determination. Vertical bars were arbitrarily drawn at 1.9 and 5.4 nS and indicate bins, or points of pooling data by MAC conductance, in *C*. *C*: relative conductance of MAC in the presence of 100 μM cytochrome *c* as a function of conductance of MAC in the absence of cytochrome *c*. Values are means ± SE; *n*, number of independent determinations. $*P < 0.05$ (Student's *t*-test).

[p*I* = 9.4 (21)]. Ribonuclease A (10–1,000 μM) reduced MAC conductance in a dose-dependent, but voltage-independent, manner, similar to the type 2 effect of cytochrome *c* (Fig. 6*A*). Typically, higher doses increase the effect, but the reduction in current is the same at positive and negative voltages. The plot of relative conductance vs. conductance of MAC reveals that the effects of ribonuclease A on MAC also depend on the initial conductance of MAC (Fig. 6, *B* and *C*). The effect of ribonuclease A was maximal when the conductance of MAC was 1.4–5.4 nS, a range almost identical to that of the effect of cytochrome *c* (Fig. 5*C*). The effect of ribonuclease A outside this range of conductance was diminished, as shown in Fig. 6*C*. Adenylate kinase (another intermembrane space protein) at 100 μM routinely disrupted the membrane patches and, therefore, could not be tested.

Sizing of MAC's pore by dextran. Nonelectrolytes, such as dextran and polyethylene glycol, are available in a variety of molecular weights and have been used to size the pores of other channels (4, 18, 19, 33, 36). When this polymer exclusion method is used for pore sizing, the conductance of the channel decreases when permeant polymers are in the bathing medium, while nonpermeant polymers have no effect. The effect on MAC activity of a series of 5% (wt/vol) 10- to 71-kDa dextrans was determined to further characterize MAC (Fig. 7). Dextran (typically 10 or 17 kDa) reduced the conductance of MAC when the estimated conductance was 1.3–5.0 nS (Fig. 7*B*). These dextrans have little effect on MAC conductance when the pore size is outside this range. These data indicate that the decrease in MAC conductance induced by dextran, like cytochrome *c* and ribonuclease A, is dependent on MAC conductance.

As expected, the reduction of MAC conductance depends on the size of the dextran molecule. As shown in Fig. 7*A*, 10-kDa dextran reduced the MAC conductance by 40% (from 4 to ~2.4 nS), whereas 17-kDa dextran only caused a ~25% decrease; 45- and 71-kDa dextrans had virtually no effect on this MAC. As shown in Fig. 7*B*, 10- and 17-kDa dextrans reduced the conductance of MAC with peak conductances of 1.3–5 nS and had little effect if the conductance was outside this range. These data suggest that the diameter of the MAC pore is slightly larger than that of 17-kDa dextran.

DISCUSSION

The onset of MAC activity in the mitochondrial outer membrane occurs early in the timeline of the apoptotic cascade, which is appropriate for a channel involved in cytochrome *c* release (30). MAC is detected 12 h after IL-3 withdrawal in parental and Bcl-2 mutant FL5.12 cells before the onset of other markers for apoptosis (Fig. 1) and is never found in Bcl-2-overexpressing cells (30). At this time, the conductance of the native outer membrane measured by directly patch clamping mitochondria increases (30), and cytochrome *c* is released (10). Furthermore, Bax is translocating into the outer membrane of mitochondria (10, 30), and the cells are beginning to decrease in size (Fig. 1). The onset of other apoptosis markers, such as annexin V and propidium iodide labeling, as well as membrane blebbing, does not begin for another 24 h (Fig. 1). Although these findings are consistent with the notion that MAC provides a pathway for cytochrome *c* early in apoptosis, the effects of cytochrome *c* on the electrophysiological properties of MAC activity provide more compelling evidence for this role of MAC in apoptosis (see below).

Investigations of the heterogeneous, but large, conductance of MAC were undertaken to further characterize this channel. The conductance of MAC is variable (Fig. 2*C*). The diameter of the pore of a channel can be estimated from the conductance using the method of Hille (Ref. 13; see MATERIALS AND METHODS). Although this method for estimating pore size is simplistic, it provides the basis for discussion of the pore size of the heterogeneous MAC. Most MAC have conductances of 1.5–5

Downloaded from http://ajpcell.physiology.org/ by 10.220.32.246 on October 13, 2017

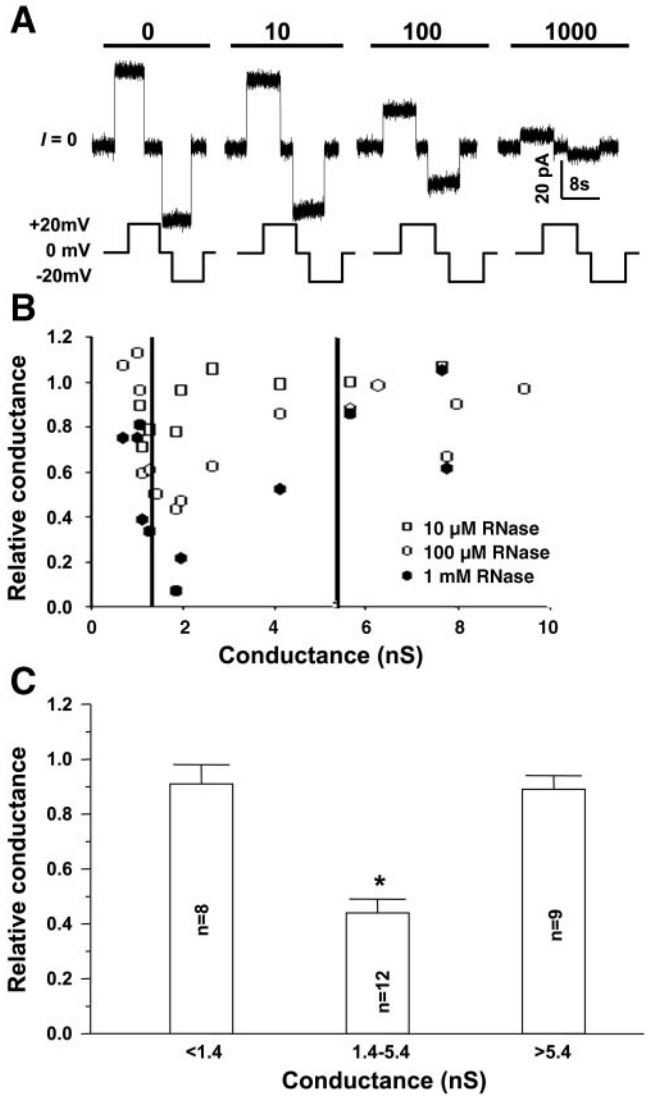

Fig. 6. Effects of ribonuclease A (RNase) on MAC. *A*: discontinuous, sequential current traces of a single patch with MAC with 2.0-nS conductance at 0–1,000 μM ribonuclease A and +20 to −20 mV at 5-kHz sampling and 2-kHz filtration. *B*: relative conductance of MAC (determined as described in Fig. 5 legend) in the presence of 10 μM, 100 μM, or 1 mM ribonuclease A plotted as a function of MAC conductance. Each point indicates a single determination. Vertical bars were arbitrarily drawn at 1.4 and 5.4 nS and indicate bins, or points of pooling data by size, in *C*. *C*: relative conductance of MAC in the presence of 100 μM or 1 mM ribonuclease A and plotted against conductance of MAC in each patch binned. Values are means ± SE; *n*, number of independent determinations. $*P < 0.001$ (Student's *t*-test). Determinations at 10 μM are not included, because this concentration does not have a statistically significant effect on MAC conductance.

nS determined from total amplitude histograms of current traces, typically at +20 mV for 30 s (Fig. 2). The thickness of the mitochondrial outer membrane is 5.1–5.8 nm (25). When the method of Hille and an average pore length of 5.5 nm are used, this conductance range corresponds to pore diameters of 2.9–5.3 nm (ignoring access resistance) and 3.6–7.6 nm (including access resistance). Cytochrome *c* is most effective in reducing the current through MAC when the conductance is 1.9–5.4 nS (Fig. 5). These conductances correspond to estimated pore diameters of 3.3–5.4 nm without and 4.1–8.1 nm with access resistance. The diameter of cytochrome *c* is 3–3.4 nm (6). Thus the MAC pore is likely large enough to permit the passage of cytochrome *c*. MAC with similar conductances responded when the pore was probed with ribonuclease A (3–3.8 nm diameter) (3) (Fig. 6).

In this study, the pore size of MAC was also estimated using dextran molecules of various sizes (Fig. 7), as has been done with other channels (18, 19). Typically, 10- and 17-kDa dextrans reduce the conductance of MAC (Fig. 7). In a few cases, 45-kDa dextran also reduces the conductance of MAC. These findings are consistent with partitioning of 10- to 17-kDa molecules, but usually not larger molecules, into the pore. The diameters of 10- and 17-kDa dextran reported in the literature are variable and have been estimated to be 2.2–6.4 and 6.9–8.2 nm, respectively (22, 33). As expected from the calculations based on the method of Hille (13), these methods indicate that MAC is permeable to 10- and 17-kDa dextrans when the estimated pore sizes are ~2.9–7.6 nm (1.5–5 nS), which is similar to the size of these dextrans. Hence, these methods suggest that the pore diameter of MAC is similar to that calculated from the conductance using the two methods of Hille.

Physiological concentrations of cytochrome *c* affect the electrophysiological properties of MAC (Figs. 3–5). The vari-

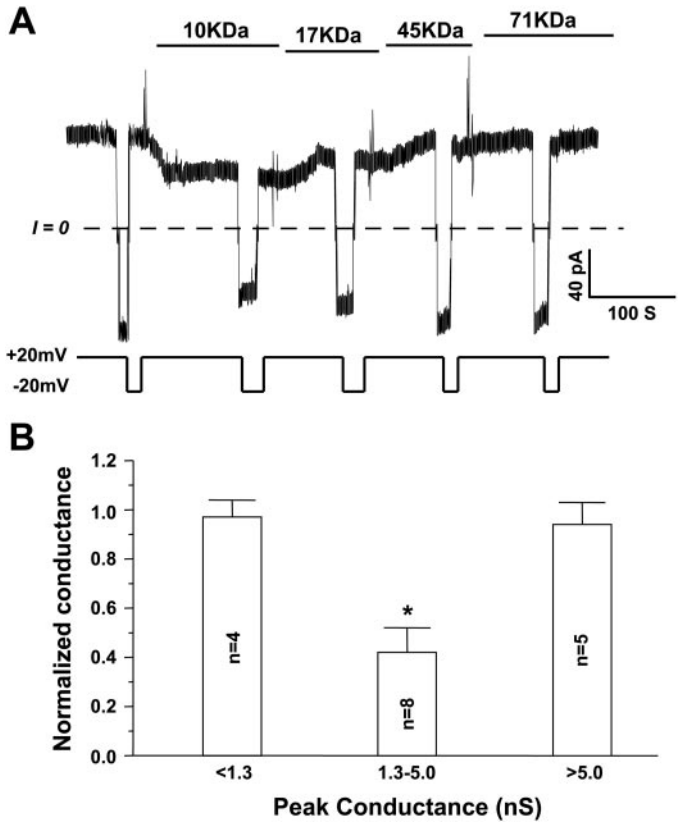

Fig. 7. Sizing of MAC by 10- to 71-kDa dextrans. *A*: current trace (5-kHz sampling and 2-kHz filtration) showing MAC with a peak conductance of ~4.0 nS during sequential perfusion of the bath with 5% (wt/vol) dextran at +20 mV, briefly at 0 mV, and −20 mV. Maximal reduction in MAC conductance was caused by 10-kDa dextran, and degree of blockade decreased as dextran size increased. *B*: MAC conductance in the presence of 10- or 17-kDa dextran normalized to that in the absence of dextran, corrected for the 14% decrease in conductivity, and grouped by conductance of MAC. Conductance of 1.3- to 5-nS MAC was reduced by 10- and 17-kDa dextran. Values are means ± SE; *n*, number of independent determinations. $*P < 0.001$ (Student's *t*-test).

Downloaded from http://ajpcell.physiology.org/ by 10.220.32.246 on October 13, 2017

ability of the extent and the reversibility of the conductance decrease suggest that more than one mechanism underlies these changes. We have classified the effects as type 1 and type 2. They occur with similar frequency and are occasionally observed in the same patch (Fig. 3, *B* and *D*).

The type 1 effect of cytochrome *c* is characterized by a modest decrease in conductance that rectifies at bath positive potentials and is reversible (Figs. 3–5). There is a consistent doubling of the noise level in the presence of physiological levels of cytochrome *c* (189 ± 24% increase in variance). All these effects are observed when charged molecules transit a pore by biochemical methods, e.g., RNA through α-hemolysin channels and ATP through VDAC (4, 14–16, 31, 32). By inference, the type 1 effects are consistent with a partitioning of these molecules into the pores and suggest that cytochrome *c* transits through MAC.

The type 2 effect of cytochrome *c* is a >50% decrease in conductance that does not rectify and is not typically reversible (Figs. 4 and 5). The type 2 effect suggests that cytochrome *c* binds to MAC in such a way that plugs the pore during transit, destabilizes the open state, or stabilizes a low-conductance state. We have not discriminated among these possibilities. However, inasmuch as the type 2 effects are not reversible 30–60 min after removal of the cytochrome *c*, destabilization of the open state or stabilization of a low-conductance state is more likely to be involved than a simple plug. Furthermore, this effect of cytochrome *c* is more pronounced when the conductance of MAC is 1.9–5.4 nS (Fig. 5, *B* and *C*). Hence, the site at which cytochrome *c* interacts with MAC may be lost and/or modified in MAC with larger pores.

Cytochrome *c* is a rather small, cationic protein that contains a heme. Several attributes of cytochrome *c* were explored to determine which were important in the reduction of MAC's conductance. The type 1 and type 2 effects are observed at high ionic strength (500 mM), suggesting that charge is not central to the blockade. Second, the heme-containing protein hemoglobin has no effect on MAC, indicating that the presence of a heme is not essential. Ribonuclease A (14 kDa) and 10- and 17-kDa dextrans similarly affect MAC conductance. Larger dextrans have no effects. Therefore, molecular size is important, while charge and the presence of a heme probably are not central to these effects.

Cytochrome *c* is released from the mitochondria of many cell types early in the apoptotic cascade. However, the mechanisms underlying cytochrome *c* release have not been established. Cytochrome *c* release can be the result of rupturing of the mitochondrial outer membrane after opening of the permeability transition pore (5, 20). However, the outer membrane of mitochondria remains apparently intact, even though cytochrome *c* has been released in some studies (2, 5, 9, 28, 30, 33, 34). In these cases, MAC may provide the transit pathway for cytochrome *c* release without compromising the integrity of the outer membrane. In previous studies, we found that proteoliposomes with MAC activity (prepared by fusion of liposomes with mitochondrial outer membranes purified from apoptotic cells) failed to retain cytochrome *c* compared with control proteoliposomes prepared from normal cells (30). This finding suggested that cytochrome *c* permeability increases early in apoptosis, when MAC is first detected. The present study represents the first report of the effects of cytochrome *c* on the electrophysiological behavior of MAC. The type 1 effects of cytochrome *c* on MAC are consistent with a partitioning of cytochrome *c* into MAC's pore. These effects are similar to those caused by ATP on VDAC (31) and single-stranded RNA on α-hemolysin channels (1, 15). In the latter study, in which RT-PCR techniques were used, RNA actually translocated through the α-hemolysin channel. The type 1 effects of cytochrome *c* on MAC activity, the enormous size of MAC's pore [which allows the partitioning of 17-kDa dextran (Fig. 7)], and our previous studies in which cytochrome *c* permeability increases in proteoliposomes expressing MAC activity (30) lend strong support to the notion that cytochrome *c* can transit the pore of MAC. Future studies should include pharmacological profiling, because MAC may represent an important novel therapeutic site for regulation of apoptosis.

ACKNOWLEDGMENTS

We thank Tom Yan and Jane McCutcheon for excellent technical assistance and Robert French (University of Calgary, Calgary, AB, Canada) for suggestions and reading the manuscript.

GRANTS

This research was supported by National Institute of General Medical Sciences Grant GM-57249 and National Science Foundation Grants MCB-0235834 and INT003797 (to K. W. Kinnally).

DISCLOSURES

Any opinions, findings, and conclusions or recommendations expressed in this study are those of the authors and do not necessarily reflect the views of the National Science Foundation (NSF) or National Institutes of Health.

Commercial names of materials and apparatus are identified only to specify the experimental apparatus. Their use does not imply a recommendation by the National Institute of Standards and Technology, New York University College of Dentistry, NSF, or National Institutes of Health, nor does it imply that they are the best available for the purpose.

REFERENCES

1. **Akeson M, Branton D, Kasianowicz JJ, Brandin E, and Deamer DW.** Microsecond time-scale discrimination among polycytidylic acid, polyadenylic acid, and polyuridylic acid as homopolymers or as segments within single RNA molecules. *Biophys J* 77: 3227–3233, 1999.
2. **Antonsson B, Conti F, Ciavatta A, Montessuit S, Lewis S, Martinou I, Bernasconi L, Bernard A, Mermod JJ, Mazzei G, Maundrell K, Gambale F, Sadoul R, and Martinou JC.** Inhibition of Bax channel-forming activity by Bcl-2. *Science* 277: 370–372, 1997.
3. **Berisio R, Sica F, Lamzin VS, Wilson KS, Zagari A, and Mazzarella L.** Atomic resolution structures of ribonuclease A at six pH values. *Acta Crystallogr D* 58: 441, 2002.
4. **Bezrukov SM and Kasianowicz JJ.** The charge state of an ion channel controls neutral polymer entry into its pore. *Eur Biophys J* 26: 471–476, 1997.
5. **Brenner C and Kroemer G.** Apoptosis. Mitochondria—the death signal integrators. *Science* 289: 1150–1151, 2000.
6. **Chan SK, Tulloss I, and Margoliash E.** Primary structure of the cytochrome *c* from the snapping turtle, *Chelydra serpentina*. *Biochemistry* 5: 2586–2597, 1966.
7. **Criado M and Keller BU.** A membrane fusion strategy for single channel recordings of membranes usually non-accessible to patch-clamp pipette electrodes. *FEBS Lett* 224: 172–176, 1987.
8. **Decker GL and Greenawalt JW.** Ultrastructural and biochemical studies of mitoplasts and outer membranes derived from French-pressed mitochondria. *J Ultrastruct Res* 59: 44–56, 1977.
9. **De Giorgi F, Lartigue L, Bauer MK, Schubert A, Grimm S, Hanson GT, Remington SJ, Youle RJ, and Ichas F.** The permeability transition pore signals apoptosis by directing Bax translocation and multimerization. *FASEB J* 16: 607–609, 2002.
10. **Gross A, Jockel J, Wei MC, and Korsmeyer SJ.** Enforced dimerization of BAX results in its translocation, mitochondrial dysfunction and apoptosis. *EMBO J* 17: 3878–3885, 1998.

Downloaded from http://ajpcell.physiology.org/ by 10.220.32.246 on October 13, 2017

11. **Gupte S and Hackenbrock C.** Multidimensional diffusion modes and collision frequencies of cytochrome *c* with its redox partners. *J Biol Chem* 263: 5241–5247, 1988.
12. **Hamill OP, Marty A, Neher E, Sakmann B, and Sigworth FJ.** Improved patch-clamp techniques for high-resolution current recording from cells and cell-free membrane patches. *Pflügers Arch* 381: 85–100, 1981.
13. **Hille B.** *Ionic Channels of Excitable Membranes (*2nd ed.). Sunderland, MA: Sinauer, 2001, p. 351–352.
14. **Kasianowicz JJ and Bezrukov SM.** Protonation dynamics of the α-toxin ion channel from spectral analysis of pH-dependent current fluctuations. *Biophys J* 69: 94–105, 1995.
15. **Kasianowicz JJ, Brandin E, Branton D, and Deamer DW.** Characterization of individual polynucleotide molecules using a membrane channel. *Proc Natl Acad Sci USA* 93: 13770–13773, 1996.
16. **Kasianowicz JJ, Henrickson SE, Weetall HH, and Robertson B.** Simultaneous multianalyte detection with a nanometer-scale pore. *Anal Chem* 73: 2268–2272, 2001.
17. **Kluck RM, Bossy-Wetzel E, Green DR, and Newmeyer DD.** The release of cytochrome *c* from mitochondria: a primary site for Bcl-2 regulation of apoptosis. *Science* 275: 1132–1136, 1997.
18. **Krasilnikov O, Sabirov R, Ternovsky V, Merzliak P, and Muratkhodjaev J.** A simple method for the determination of the pore radius of ion channels in planar lipid bilayer membranes. *FEMS Microbiol Immunol* 105: 93–100, 1992.
19. **Krasilnikov OV.** Sizing channels with neutral polymers. In: *Structure and Dynamics of Confined Polymers*, edited by Kasianowicz JJ, Kellermayer MSZ, and Deamer DW. Dordrecht: Kluwer Academic, 2002, p. 97–116.
20. **Kroemer G and Reed JC.** Mitochondrial control of cell death. *Nat Med* 6: 513–519, 2000.
21. **Lee HG and Desiderio DM.** Optimization of the capillary zone electrophoresis loading limit and resolution of proteins, using triethylamine, ammonium formate and acidic pH. *J Chromatogr B Biomed Appl* 691: 67–75, 1997.
22. **Leypoldt JK and Henderson LW.** Molecular charge influences transperitoneal macromolecule transport. *Kidney Int* 43: 837–844, 1993.
23. **Liu X, Kim CN, Yang J, Jemmerson R, and Wang X.** Induction of apoptotic program in cell-free extracts: requirement for dATP and cytochrome *c*. *Cell* 86: 147–157, 1996.
24. **Lohret TA, Jensen R, and Kinnally KW.** The Tim23 import protein is required for normal activity of a mitochondrial inner membrane channel. *J Cell Biol* 137: 377–386, 1997.
25. **Mannella CA.** Structure of the outer mitochondrial membrane: analysis of X-ray diffraction from the plant membrane. *Biochim Biophys Acta* 645: 33–40, 1981.
26. **Mannella CA.** Structure of the outer mitochondrial membrane: ordered arrays of pore-like subunits in outer membrane fractions from *Neurospora crassa* mitochondria. *J Cell Biol* 94: 680–687, 1982.
27. **Mannella CA, Guo XW, and Cognon B.** Diameter of the mitochondrial outer membrane channel: evidence from electron microscopy of frozen-hydrated membrane crystals. *FEBS Lett* 253: 231–234, 1989.
28. **Martinou JC and Green DR.** Breaking the mitochondrial barrier. *Nat Rev Mol Cell Biol* 2: 63–66, 2001.
29. **Oltvai ZN, Milliman CL, and Korsmeyer SJ.** Bcl-2 heterodimerizes in vivo with a conserved homolog, Bax, that accelerates programmed cell death. *Cell* 74: 609–619, 1993.
30. **Pavlov EV, Priault M, Pietkiewicz D, Cheng EHY, Antonsson B, Manon S, Korsmeyer SJ, Mannella CA, and Kinnally KW.** A novel, high conductance channel of mitochondria linked to apoptosis in mammalian cells and Bax expression in yeast. *J Cell Biol* 155: 725–732, 2001.
31. **Rostovtseva TK and Bezrukov SM.** ATP transport through a single mitochondrial channel, VDAC, studied by current fluctuation analysis. *Biophys J* 74: 2365–2373, 1998.
32. **Rostovtseva TK, Komarov A, Bezrukov SM, and Colombini M.** Dynamics of nucleotides in VDAC channels: structure-specific noise generation. *Biophys J* 82: 193–205, 2002.
33. **Saito M, Korsmeyer SJ, and Schlesinger PH.** BAX-dependent transport of cytochrome *c* reconstituted in pure liposomes. *Nat Cell Biol* 2: 553–555, 2000.
34. **Shimizu S, Matsuoka Y, Shinohara Y, Yoneda Y, and Tsujimoto Y.** Essential role of voltage-dependent anion channel in various forms of apoptosis in mammalian cells. *J Cell Biol* 152: 237–250, 2001.
35. **Tanford C.** Molecular structure. In: *Physical Chemistry of Macromolecules.* New York: Wiley, 1961, p. 57–60.
36. **Truscott K, Kovermann P, Geissler A, Merlin A, Meijer M, Driessen A, Rassow J, Pfanner N, and Wagner R.** A presequence- and voltage-sensitive channel of the mitochondrial preprotein translocase formed by Tim23. *Nat Struct Biol* 8: 1074–1082, 2001.
37. **Wei MC, Zong WX, Cheng EH, Lindsten T, Panoutsakopoulou V, Ross AJ, Roth KA, MacGregor GR, Thompson CB, and Korsmeyer SJ.** Proapoptotic BAX and BAK: a requisite gateway to mitochondrial dysfunction and death. *Science* 292: 727–730, 2001.
38. **Yang J, Liu X, Bhalla K, Kim CN, Ibrado AM, Cai J, Peng TI, Jones DP, and Wang X.** Prevention of apoptosis by Bcl-2: release of cytochrome *c* from mitochondria blocked. *Science* 275: 1129–1132, 1997.
39. **Yin XM, Oltvai Z, and Korsmeyer SJ.** BH1 and BH2 domains of Bcl-2 are required for inhibition of apoptosis and heterodimerization with Bax. *Nature* 369: 272–273, 1994.

Downloaded from http://ajpcell.physiology.org/ by 10.220.32.246 on October 13, 2017